Supplementary information

A compact interphase involving reversible redox couple stabilizes 4.6 V $LiCoO_2$ cathode

Junbo Zhang[1,2], Chengwu Liu[3], Haikuo Zhang[2], Ruhong Li[2], Ling Lv[2], Di Lu[2], Shuoqing Zhang[2], Xuezhang Xiao[2], Shujiang Geng[1], Fuhui Wang[1], Tao Deng[4], Lixin Chen[2,5], and Xiulin Fan[2]*

1 *Shenyang National Laboratory for Materials Science, Northeastern University, Shenyang, 110819, China.*

2 *State Key Laboratory of Silicon Materials, School of Materials Science and Engineering, Zhejiang University, Hangzhou 310027, China.* xlfan@zju.edu.cn

3 *Department of Chemical Engineering, Shanghai Electrochemical Energy Devices Research Center, Shanghai Jiao Tong University, Shanghai 200240, China.*

4 *Department of Chemical and Biomolecular Engineering, University of Maryland, College Park, MD, USA.*

5 *Key Laboratory of Advanced Materials and Applications for Batteries of Zhejiang Province, Hangzhou 310013, China.*

Experimental Methods

Materials

Lithium metal foil (15.6 mm diameter, and 500 μm thick) was purchased from China Energy Lithium Co., Ltd. $LiCoO_2$ (LCO), graphite, and carbon black were purchased from Kelude Co, Ltd. Battery-grade EC, DMC, FEC, $LiPF_6$, polyvinylidene fluoride (PVDF), N-methyl pyrrolidone (NMP), lithium hydroxide (LiOH), and polyacrylic acid (PAA) were purchased from Duoduo Chem Co., Ltd. All solvents were dried by molecular sieves to a residual water concentration of less than 10 ppm (measured by Karl–Fisher titration).

Preparation of electrolytes and electrodes

Two kinds of electrolytes (1 M $LiPF_6$/EC–DMC (1:1 by vol) (BE) and 1 M $LiPF_6$/EC–DMC (1:1 by vol)+1 *wt*% FEC (BE+FEC)) were used as reference electrolytes. The 1 M $LiPF_6$/EC–DMC+0.5 *wt*% BFS (BE+BFS) electrolyte was obtained by mixing BFS into the BE. All the above processes were carried out in a glovebox filled with purified argon, where the moisture and oxygen contents were <0.01 ppm. For coin cells, LCO electrodes were prepared by slurry coating using NMP as the solvent. The slurry contained the active material (LCO), carbon black, and PVDF binder in a weight ratio of 8:1:1. The resulting slurry was deposited on Al foil and then dried at 80 °C for 12 h under vacuum. After that, the electrodes were punched into discs and stored in a purified argon-filled glovebox. A typical loading of cathode active materials on the post-drying electrode is ~1.5 mAh cm^{-2}. The graphite electrode was processed by a similar method, using deionized water as the solvent; it contained 93 *wt*. % graphite, 2 *wt*. % carbon black, and 5 *wt*. % LiPAA (from a 10 *wt*. % aqueous solution) binder. The resulting slurry was coated on Cu foil. A typical loading of anode active materials was ~1.8 mAh cm^{-2}. The negative-to-positive capacity ratio (N/P) of the assembled full cells was around 1.2.

For graphite||LCO pouch cells, the active material loading of the graphite anode and LCO cathode was 96.7% and 98.6%, respectively. The press density of the graphite anode and LCO cathode was 1.7 g cc^{-1} and 4.1 g cc^{-1}, respectively. The N/P ratio was

~1.1.

Electrochemical measurements

All coin cells (2025-type) were assembled with one piece of polyethylene separator (Celgard2400) and 75 μL electrolyte in an argon-filled glove box if not specially indicated. For the 1-Ah pouch cell, 2 g electrolyte was injected to pursue a higher energy density. Galvanostatic charge–discharge cycling and rate performances of cells were conducted on a Landt battery cycler (Wuhan LAND Electronics Co., Ltd.). All cells were activated at a rate of 0.1 C for 3 cycles and then operated in the corresponding potential range for the subsequent cycles (Li||LCO: 3–4.6 V, graphite||LCO: 3–4.55 V) if not specially indicated. For GITT tests, cells were cycled at a rate of C/3 with a 12 min pulse time and a 5-h rest time (after 100 cycles at 0.5 C charge and 1 C discharge rates). The electrochemical floating tests were performed in coin cells with LCO and Li metal as the cathode and anode, respectively. The cells were charged to 5 V and then maintained at this voltage for 12 h with their current monitored. The electrochemical stability of the electrolytes was evaluated by a linear sweep voltammetry method at a scan rate of 1 mV s^{-1} using a Li||Al configuration. EIS measurements were carried out using an electrochemical workstation with an amplitude of 10 mV over a frequency range from 10 kHz to 0.01 Hz. LSV and EIS tests were conducted on Ivium electrochemical workstation (The Netherlands). The above electrochemical tests were run at 25 °C.

Characterization

For sample post-analysis, including SEM, Cryo-TEM, and XPS measurements, cycled coin cells were disassembled inside an argon-filled glovebox to collect the cathodes and anodes. These electrodes were rinsed with DMC to remove any residual electrolyte and dried for further characterizations. SEM was performed with a Hitachi SU-70 microscope at 3 kV. Cryo-TEM was carried out by a JEOL JEM-ARM200 aberration-corrected microscope at 200 kV. XPS measurements were conducted in a Thermo Scientific ESCALAB 250Xi scanning X-ray microprobe with a monochromatic Al Kα X-ray (1,486.6 eV) source. X-ray diffraction patterns were obtained on a Rigaku

MiniFlex II X-ray diffraction (XRD) instrument (Cu Ka radiation, 30 kV, 15 mA, and scan rate 0.3° min^{-1}). The transition-metal (Co) dissolution of the fully charged LCO cathodes (disassembled from graphite||LCO full cells after 100 cycles at 0.5 C charge and 1 C discharge rates) was determined by inductively coupled plasma mass spectrometry (ICP-MS, Agilent 7700).

Theoretical calculations

The adsorption of different solvents on LCO cathode was performed using the projector-augmented wave (PAW) method implanted in the Vienna ab-initio Simulation Package (VASP). The Perdew-Burke-Ernzerhof (PBE) functional with the generalized gradient approximation (GGA) exchange correlation was employed to describe the exchange-correlation interactions. The wave functions were expanded by using the plane-wave energy cutoff of 550 eV. Brillouin-zone integrations were approximated by using special k-point sampling of Monkhorst-Pack scheme with a k-point mesh of 1 × 2 × 1. All the configurations are fully relaxed until the total energy are less than 1×10^{-5} eV $atom^{-1}$ and the force on each atom are less than 0.01 eV $Å^{-1}$. The adsorption energies of different solvents on LCO cathode were determined by the formula: $E_{ads}=E_{sub/s}-E_s-E_{sub}$, where E_{sub} is the total energy of the surface (104) of $Li_{36}Co_{48}O_{96}$ with a 20 Å vacuum layer; E_s is the total energy of different solvents; $E_{sub/s}$ is the total energy of solvents absorbed on the surface (104) of $Li_{36}Co_{48}O_{96}$. A DFT-D3 method was used to describe the van der Waals interactions.

The energies of the highest occupied molecular orbital (HOMO) and lowest unoccupied molecular orbital (LUMO) were calculated by the Gaussian 09 software. Molecules, including EC, DMC, FEC, VC, BFS, and $LiPF_6$, were firstly optimized with three-parameter empirical formulation B3LYP in conjunction with the basis set of 6-311+G(d, p) under the gas phase approximation [1,2]. Then, self-consistent calculations were conducted to obtain the energies of HOMO and LUMO.

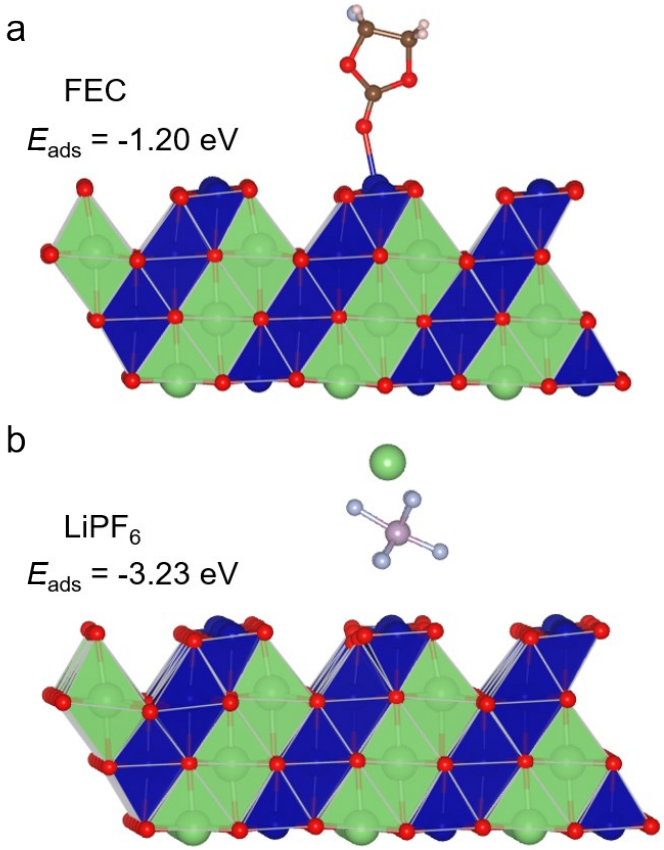

Supplementary Fig. 1 Adsorption energies of the FEC (a) and $LiPF_6$ (b) on the (104) surface of LCO cathode.

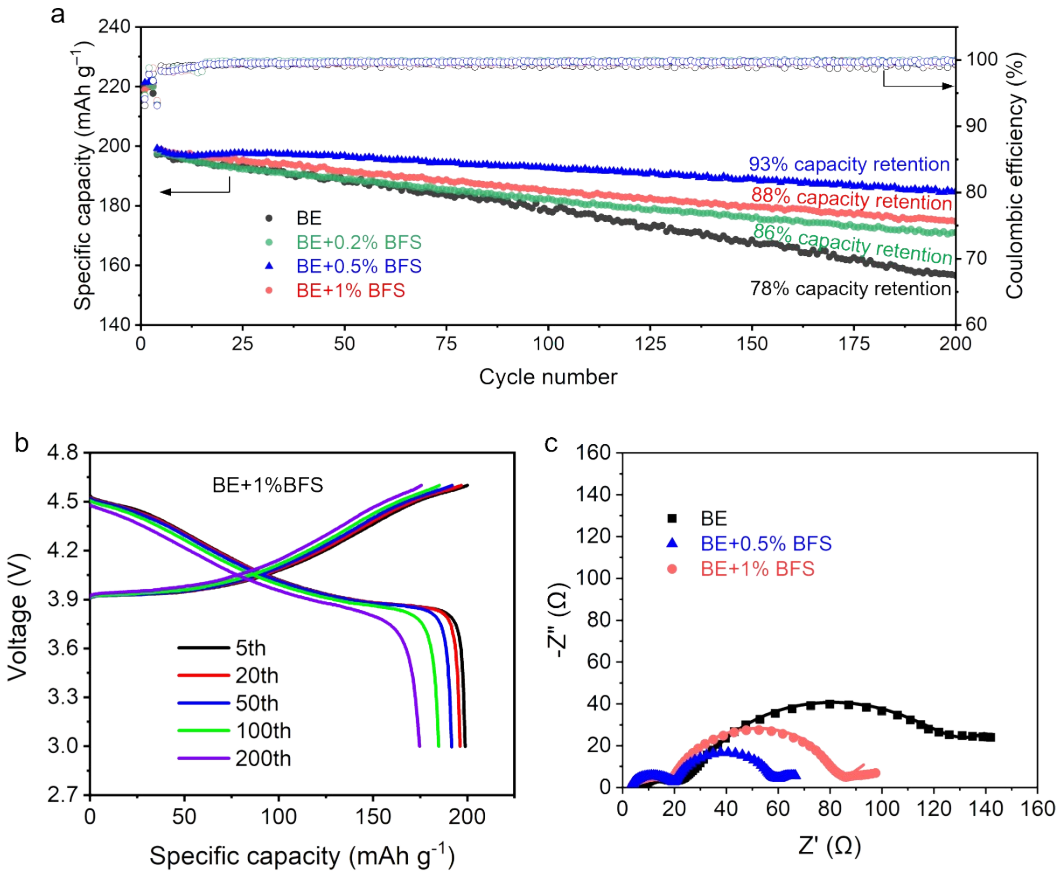

Supplementary Fig. 2 Systematic screening of the electrolyte formulation with an optimum ratio. (a), Long-term cycling stability of Li||LCO cells using different electrolytes. (b), Galvanostatic charge-discharge curves of 4.6 V Li||LCO cells using the BE+1% BFS. (c), Electrochemical impedance spectroscopy results of Li||LCO cells after 200 cycles with different electrolytes.

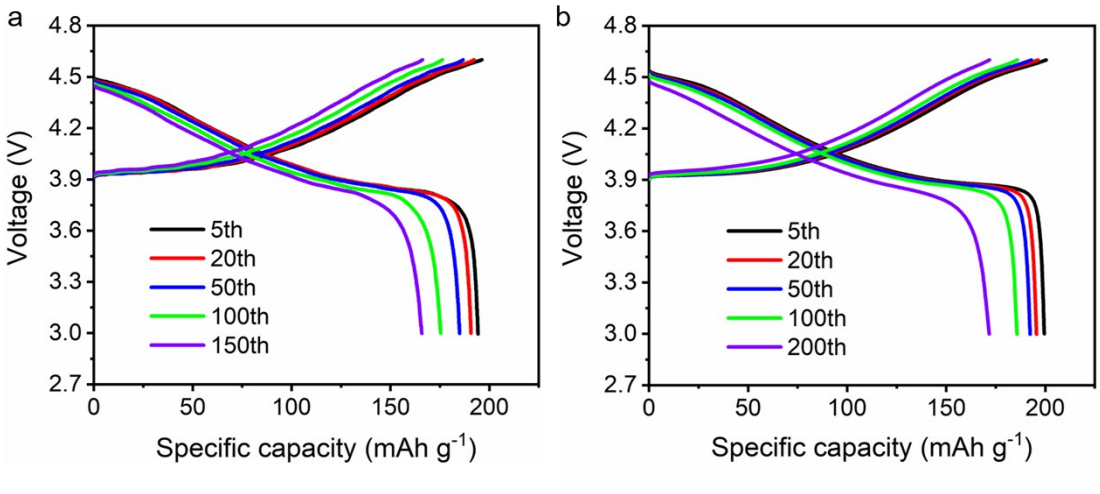

Supplementary Fig. 3 Galvanostatic charge-discharge curves of 4.6 V Li||LCO cells using the BE (a) and BE+FEC (b).

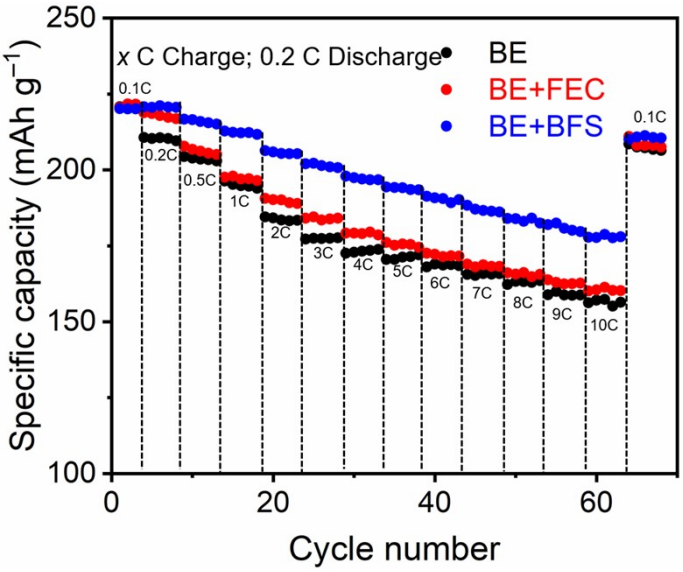

Supplementary Fig. 4 Rate performance of 4.6 V Li||LCO cells using different electrolytes at varied charge and 0.2 C discharge rates.

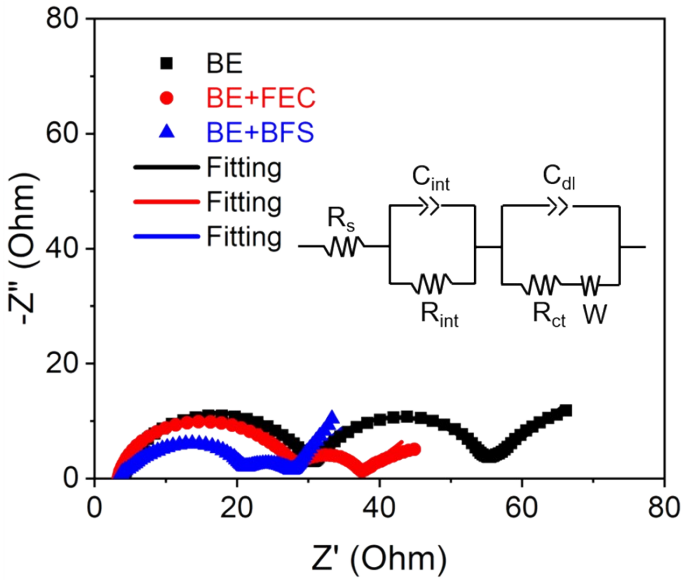

Supplementary Fig. 5 EIS of uncycled Li||LCO cells with different electrolytes. Inset shows the fitted equivalent circuit.

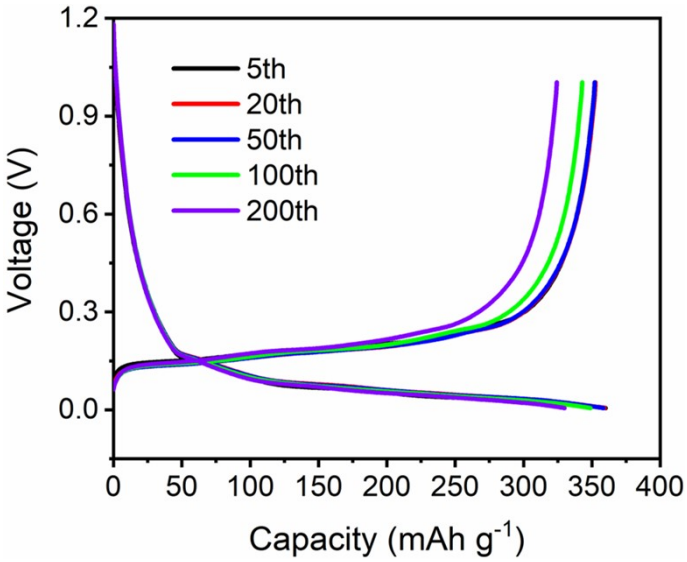

Supplementary Fig. 6 Galvanostatic charge-discharge curves of Li||graphite cells using BE.

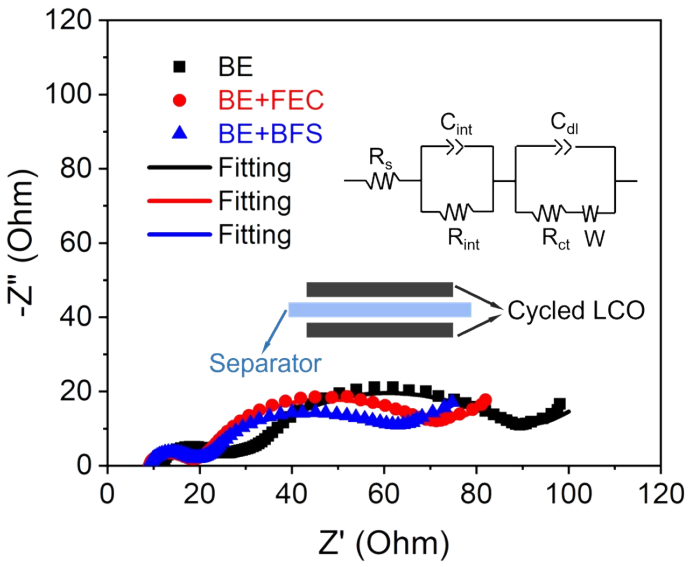

Supplementary Fig. 7 EIS of the LCO||LCO symmetric cells using LCO cathodes retrieved from the graphite||LCO cells after 100 cycles.

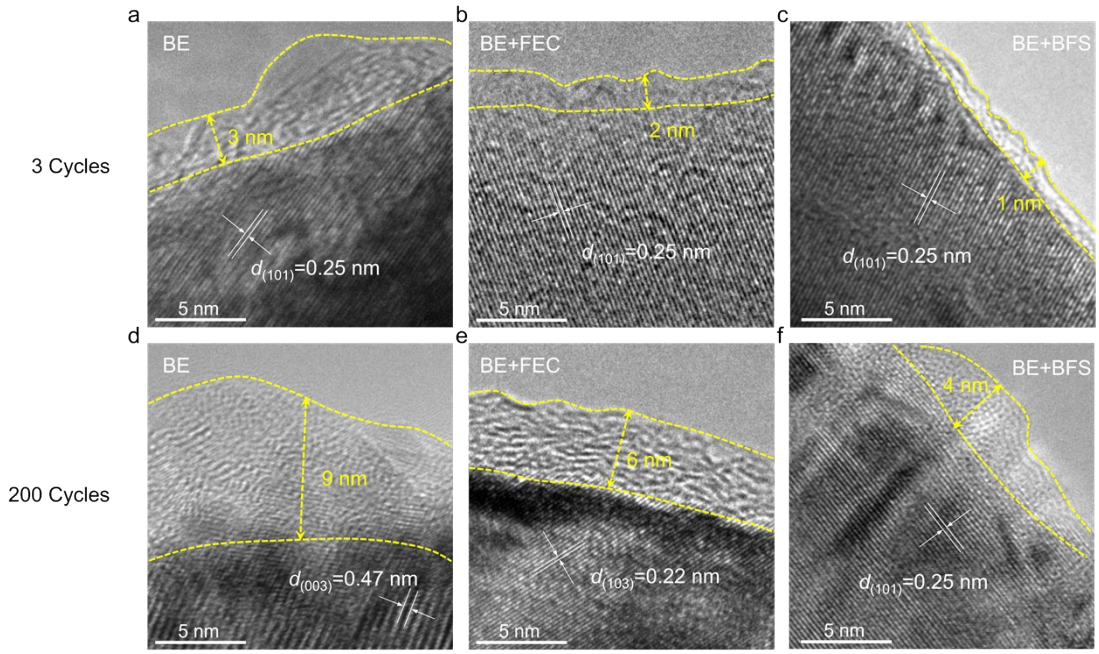

Supplementary Fig. 8 TEM images of LCO cathodes retrieved from Li||LCO cells after different cycles in BE (a, d), BE+FEC (b, e) and BE+BFS (c, f) electrolyte.

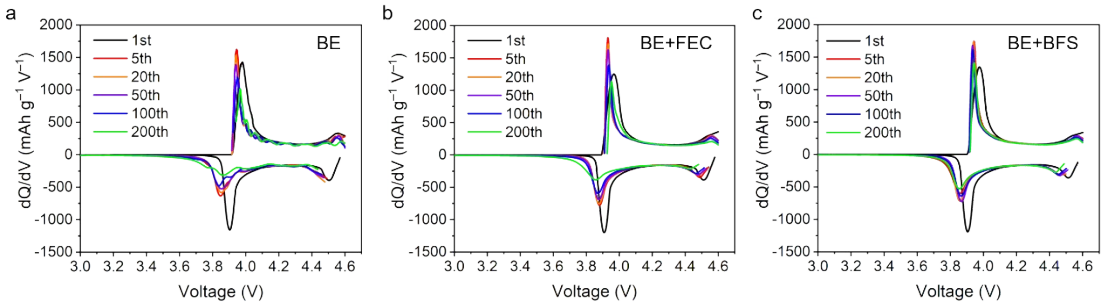

Supplementary Fig. 9 dQ/dV curves of Li||LCO cells at the selected cycles in BE (a), BE+FEC (b), and BE+BFS (c) electrolyte based on the charge/discharge profiles presented in Fig. 2a, b, and Supplementary Fig. 3.

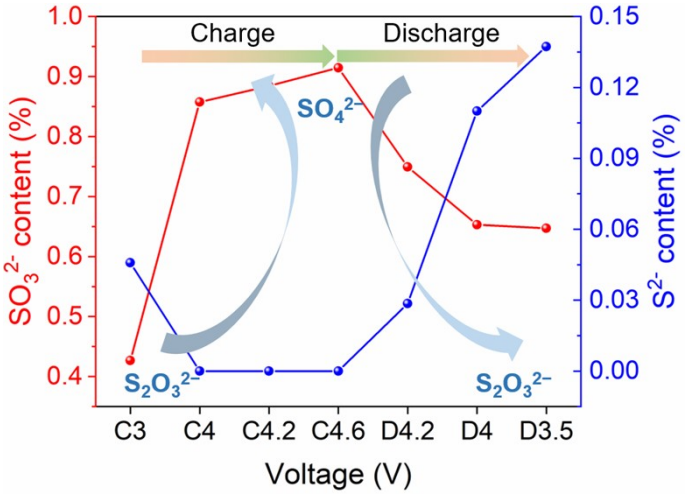

Supplementary Fig. 10 Relative ratios of SO_4^{2-} and $S_2O_3^{2-}$ during the second charge−discharge process of the LCO cathode cycled in the BE+BFS obtained from XPS results.

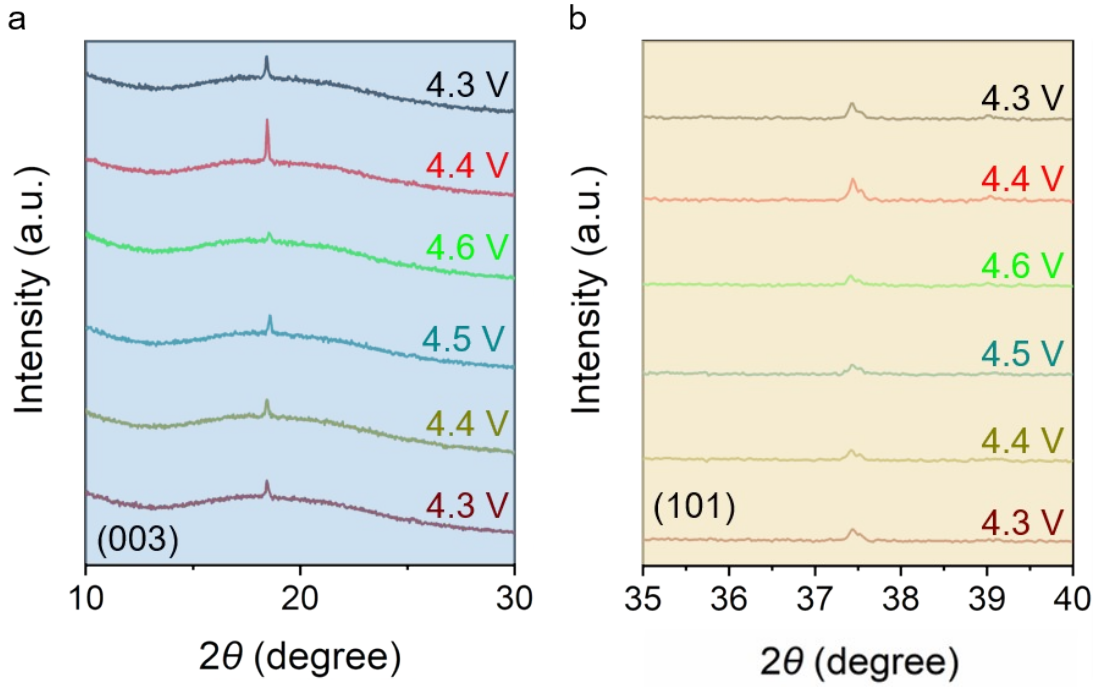

Supplementary Fig. 11 The ex situ XRD patterns evolution in selected region of the (003) planes (a) and (101) planes (b) of LCO cathode collected during the charge/discharge process with the BE+BFS under 0.1 C.

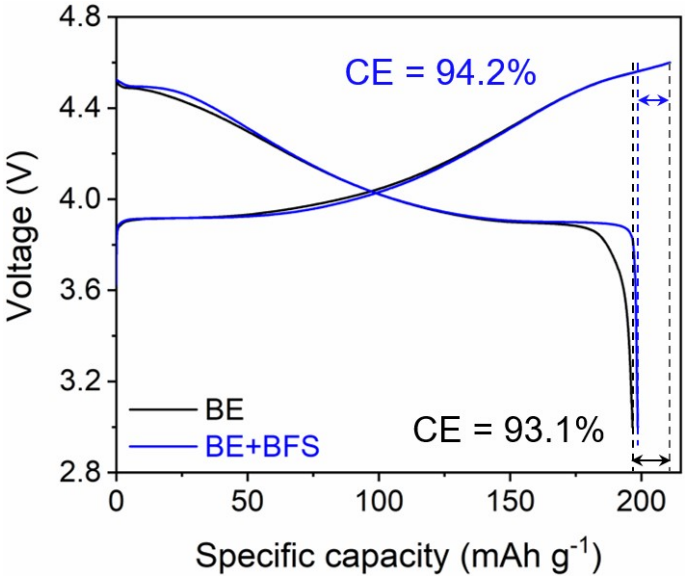

Supplementary Fig. 12 Recoverable capacity from fully charged Li||LCO cells in different electrolytes after resting 24 hours.

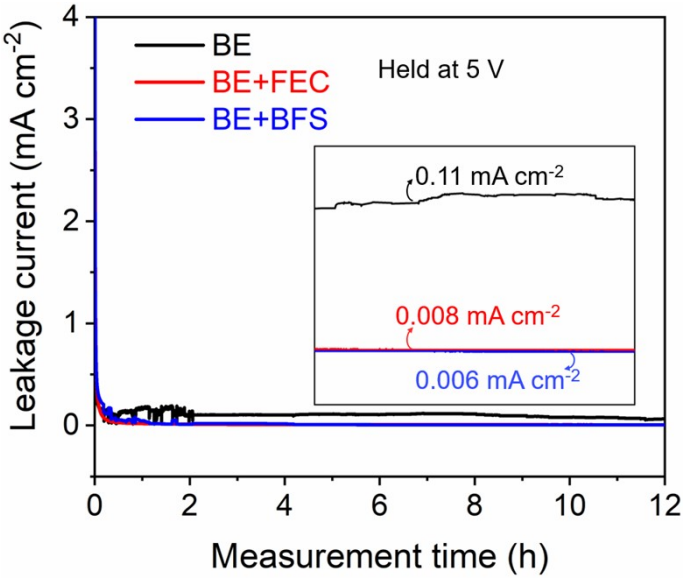

Supplementary Fig. 13 Leakage currents during a constant-voltage (5 V vs. Li^+/Li) floating test of the LCO cathodes after 3 cycles in different electrolytes.

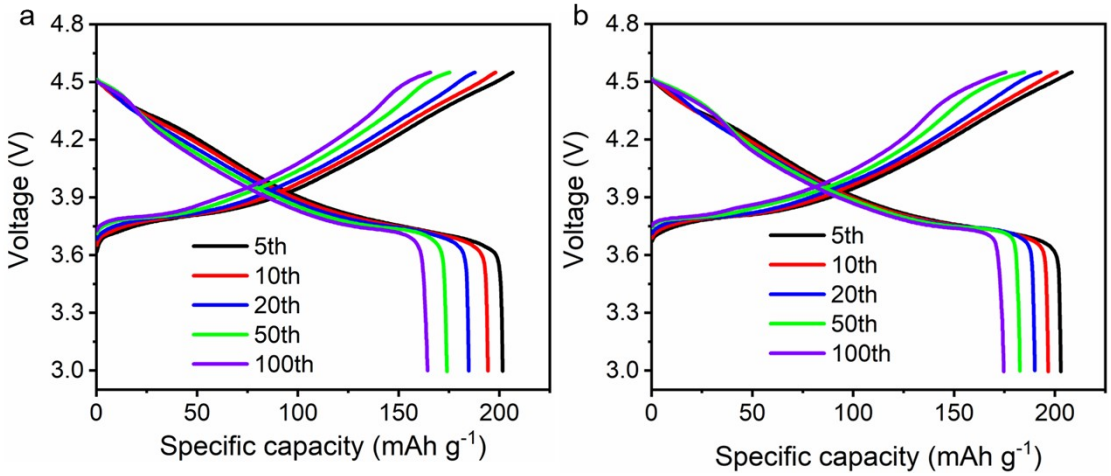

Supplementary Fig. 14 Voltage-capacity profiles of graphite||LCO full cells using BE (a) and BE+FEC (b) electrolytes at 0.5 C charge and 1 C discharge in the voltage range of 3-4.55 V.

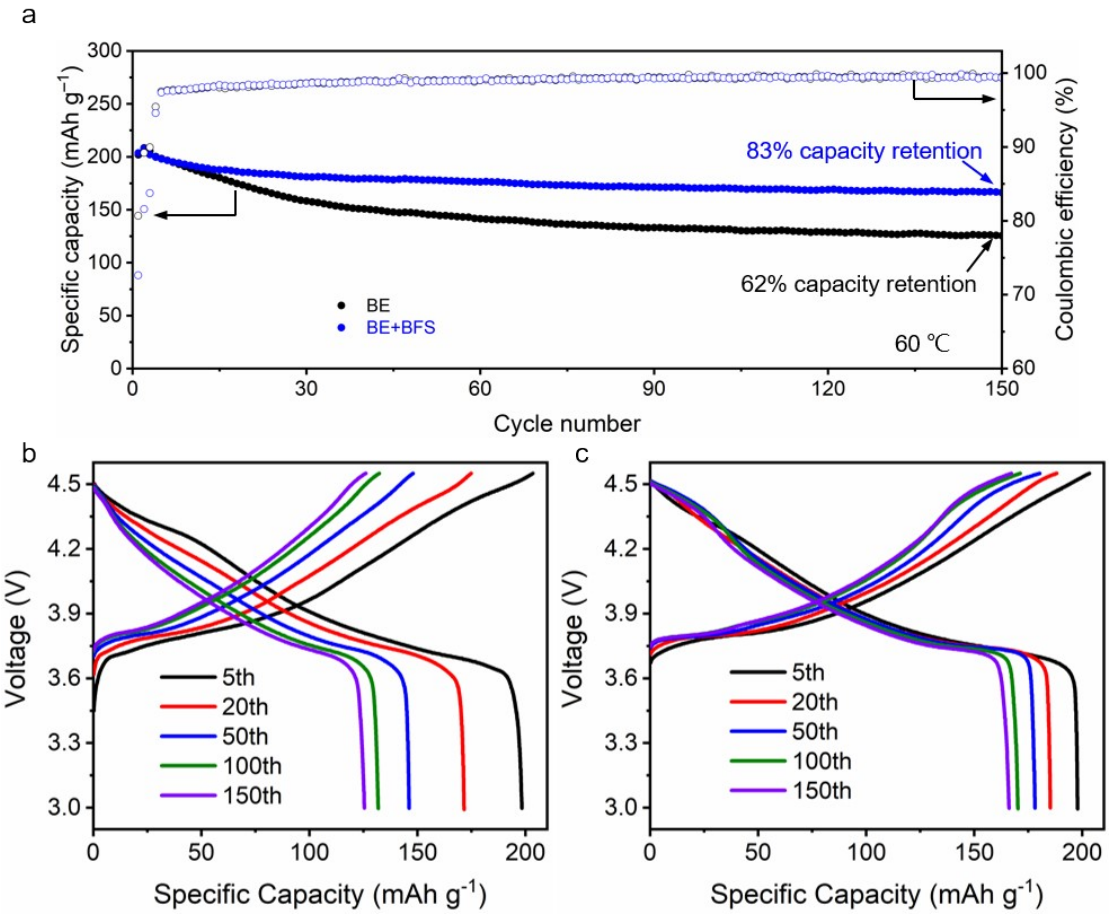

Supplementary Fig. 15 High-temperature (60 ℃) cycling stability of 4.55 V graphite||LCO cells with different electrolytes at 0.5C charge/1C discharge after 3 activation cycles at 0.1C (a) and corresponding galvanostatic charge-discharge curves of graphite||LCO cells using the BE (b) and BE+BFS (c).

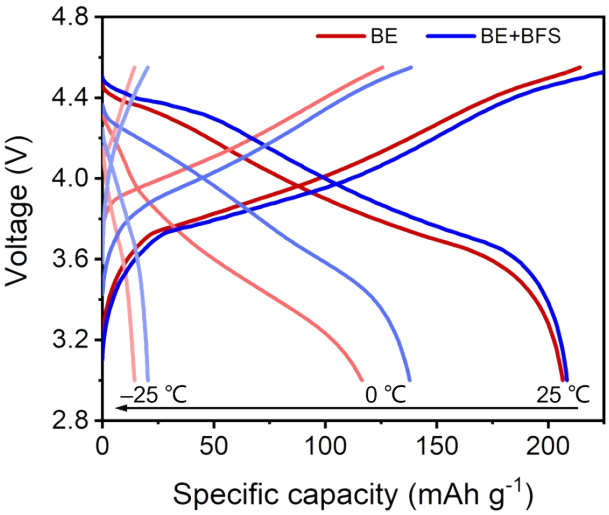

Supplementary Fig. 16 Galvanostatic charge-discharge curves of 4.55 V graphite||LCO cells at low-temperature (0 ℃ and −25 ℃) with 0.3 C charge/discharge rate.

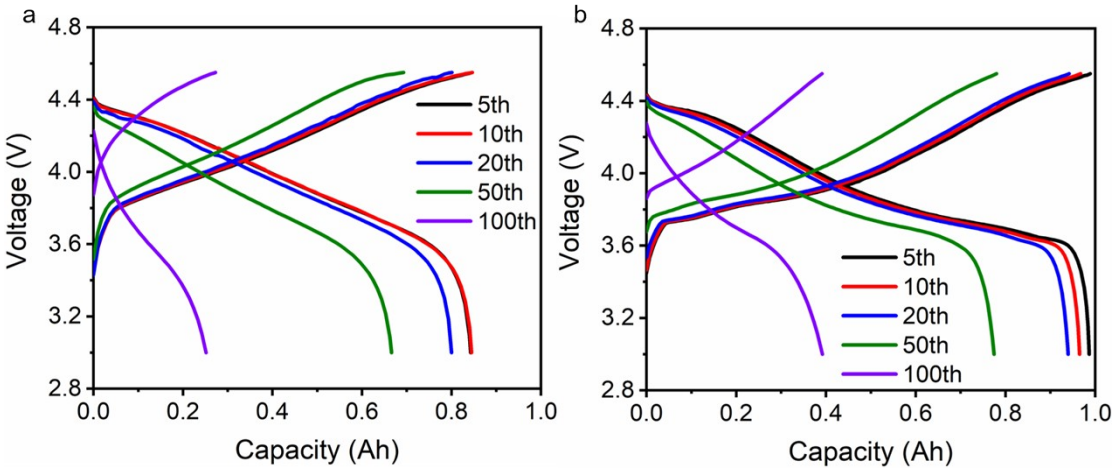

Supplementary Fig. 17 Voltage-capacity profiles of 1 Ah-level graphite||LCO pouch cells using BE (a) and BE+FEC (b) electrolytes in the voltage range of 3-4.55 V.

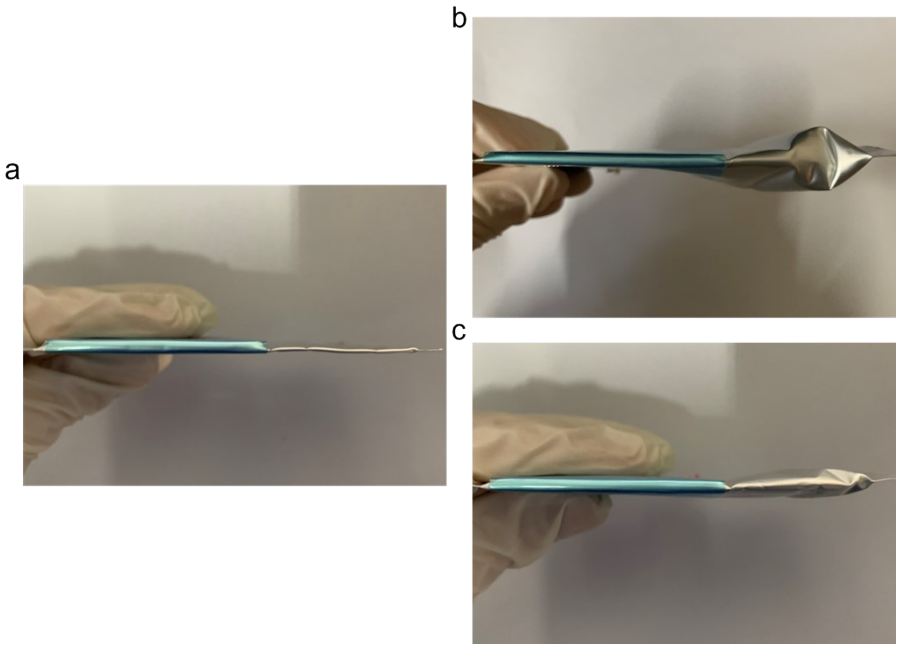

Supplementary Fig. 18 Optical images of gas expansion in graphite||LCO pouch cells. a, Pristine graphite||LCO pouch cell. b, The graphite||LCO pouch cell after 100 cycles in BE. c, The graphite||LCO pouch cell after 100 cycles in BE+BFS.

Supplementary Table 1 Physicochemical properties of different electrolytes.

Electrolytes	Viscosity (mPa·s) (25℃)	Ionic conductivity (mS/cm) (25℃)
BE	3.1649	10.16
BE+FEC	3.1655	10.23
BE+BFS	3.1652	10.39

Supplementary Table 2 The fitted electrolyte resistance (R_s), interfacial resistance (R_{int}) and charge-transfer resistance (R_{ct}) for uncycled Li||LCO cells and Li||LCO cells after 300 cycles, respectively.

Cycles	Electrolytes	R_s/Ω	R_{int}/Ω	R_{ct}/Ω	R_{int}+R_{ct}/Ω
0 cycles	BE	4.2	25.9	23.2	49.1
	BE+FEC	3.9	23.3	8.2	31.5
	BE+BFS	3.6	18.1	4.3	22.4
300 cycles	BE	5.4	90.1	360.5	450.6
	BE+FEC	5.4	62.7	63.3	126
	BE+BFS	5.3	28.6	54.2	82.8

Supplementary Table 3 The fitted electrolyte resistance (R_s), interfacial resistance (R_{int}) and charge-transfer resistance (R_{ct}) for LCO||LCO symmetric cells using LCO cathodes retrieved from the graphite||LCO cells after 100 cycles.

Electrolytes	R_s/Ω	R_{int}/Ω	R_{ct}/Ω	(R_{int}+R_{ct})/Ω
BE	10.64	17.54	60.29	77.83
BE+FEC	8.806	11.37	49.38	60.75
BE+BFS	8.503	9.61	41.88	51.49

Supplementary Table 4 Parameters of graphite||LCO pouch cells with 315 Wh kg^{-1} at 1-Ah level.

Graphite||LCO	Parameter	Value
		1 Ah-level
LCO cathode	Discharge capacity	220 mAh g^{-1}
	Active material loading	98.6%
	Press density	4.1 g cc^{-1}
	Areal wight	18.7 mg cm^{-2}
	Number of layers	9
	Total mass	5.3 g
Graphite	Discharge capacity	372 mAh g^{-1}
	Active material loading	96.7%
	Press density	1.7 g cc^{-1}
	Areal wight	12 mg cm^{-2}
	N/P ratio	1.1
	Total mass	3.4 g
Al current	Thickness	7 μm
	Total mass	0.34 g
Cu current	Thickness	6 μm
	Total mass	0.84 g
Electrolyte	E/C ratio	2 g $(Ah)^{-1}$
	Total mass	2 g
Separator	Total mass	0.0005 g
Tab	Total mass	0.1 g
Package	Total mass	1.15 g
Cell	Average voltage	4.13 V
	Energy density	315 Wh kg^{-1}

Note: Energy density calculation method:

The total weight of graphite||LCO pouch cell is 13.1 g. The average output voltage is 4.13 V. The calculated energy density of the cell is 315 Wh kg^{-1} (=1 Ah*4.13 V/ 0.0131 kg).

References

1. Austin, A. et al. Density functional with spherical atom dispersion terms. *J. Chem. Theory Comput.* **8**, 4989-5007 (2012).
2. Peverati, R., & Truhlar, D.G. M11-L: A local density functional that provides improved accuracy for electronic structure calculations in chemistry and physics. *J. Phys. Chem. Lett.* **3**, 117-124 (2012).